Journal of Applied Electrochemistry **33**: 627–633, 2003.

Electrodeposition of noncrystalline cobalt–tungsten alloys from citrate electrolytes

M.A.M. IBRAHIM*, S.S. ABD EL REHIM and S.O. MOUSSA
Department of Chemistry, Faculty of Science, Ain Shams University, Cairo, Egypt
*(*author for correspondence, e-mail: imagdy1963@hotmail.com)*

Received 16 October 2002; accepted in revised form 25 March 2003

Key words: citrate baths, cobalt–tungsten, codeposition, non-crystalline alloy, potentiodynamic

Abstract

Induced electrodeposition of Co–W alloys onto steel substrates from acid citrate baths has been investigated. The effects of some plating parameters, such as current density, pH and temperature on the potentiodynamic cathodic polarization curves, cathodic current efficiency of the alloy and the percentage tungsten in the alloy were studied. Highly adherent and compact Co–W alloys codeposited from citrate baths containing up to 28 mass % tungsten were obtained. The percentage W (w/w) in the alloy increases with increasing pH, bath temperature and Co^{2+} ion concentration. On the other hand, the percentage W in the alloy decreases with increasing current density. Anodic linear stripping voltammetry (ALSV) indicated that the alloy might consist of one phase solid solution. These alloys were determined to be noncrystalline by X-ray diffraction analysis.

1. Introduction

Cobalt–tungsten alloys are of interest due to their exceptional hardness, wear resistance [1] and high corrosion resistance [2, 3]. Moreover, due to the high hardness of tungsten alloys, they can successfully substitute hard chromium coatings, which are formed in the environmentally hazardous process based on hexavalent chromium [4]. Many investigations have been devoted to electrodeposition of tungsten with iron-group metals from different baths [2, 5–13]. However, the mechanism of tungsten alloy electrodeposition has still not been elucidated. Indeed, tungsten metal has never been deposited in a pure state from aqueous solutions, whereas its codeposition with iron-group metals is possible [2]. Several hypotheses have been proposed and the most acceptable is that of Holt et al. [14, 15]. They postulated that initially an oxide of tungsten is deposited on the cathode and is subsequently reduced by atomic hydrogen. The role of the iron-group metal is to catalyse the reduction of the oxide to tungsten.

The aim of the present study was to investigate the process of electrodeposition of cobalt-tungsten alloys, from acid citrate baths, clarifying the factors influencing tungsten content. Citrate electrolytes are particularly attractive because they do not pollute the environment and are nontoxic. Moreover, in some cases, citrate can function as brightening [16], levelling [17] and buffering agent [18], thus eliminating the need for other bath additives.

2. Experimental details

Experiments were carried out in baths containing cobalt sulfate ($CoSO_4 \cdot 7H_2O$), sodium tungstate ($Na_2WO_4 \cdot 2H_2O$), citric acid ($C_6H_8O_7$) and tri-sodium citrate ($Na_3C_6H_5O_7$). All the plating baths and reagents used were made from analytical grade chemicals and doubly distilled water. The compositions of some baths examined for Co–W alloy codeposition are given in Table 1. For electrodeposition, a steel cathode and platinum sheet anode both of dimensions 2.5 cm × 3.0 cm were used. The plating cell used was a rectangular Perspex trough provided with vertical grooves, on each of the side walls, to fix the electrodes. Before each run, the steel cathode was mechanically polished with different grade emery papers (600, 800, 1000 and 1200) and then washed with distilled water, rinsed with ethanol and weighed. Direct current was supplied by a d.c. power supply unit (GPS-3030 D). The percentage cathodic current efficiencies, CCE%, of the alloy were determined from the mass and compositions of the deposited alloy and the charge passed [2]. The composition of the alloy was determined by electron dispersive X-ray spectrometry, EDX (Cambridge Scanning Company Ltd). The plating duration was 20 min. A potentiostat / galvanostat (EG & G, model 273) controlled by PC was used for the potentials and the stripping voltammetric measurements. All potentials were measured relative to a saturated calomel electrode (SCE). To avoid contamination, the reference electrode was connected to the working steel cathode via bridge provided

Table 1. Composition of some baths used

Bath number	$[CoSO_4 \cdot 7H_2O]$ /mol dm^{-3}	$[Na_2WO_4 \cdot 2H_2O]$ /mol dm^{-3}	$[C_6H_8O_7]$ /mol dm^{-3}	$[Na_3C_6H_5O_7]$ /mol dm^{-3}	pH
Co-1	0.2	–	0.04	0.25	5
W-1	–	0.05	0.04	0.25	5
(Co–W)*	0.2	0.05	0.04	0.25	5

with a Luggin–Haber tip and filled with the solution under test. The capillary was placed as near as possible to the cathode surface.

Potentiodynamic anodic linear stripping voltammetric (ALSV) investigations were carried out in a cell containing a platinum sheet cathode (2.5 cm × 3.0 cm) as working electrode, a saturated calomel reference electrode and a platinum wire as counter electrode. Codeposition of Co–W from the plating bath was carried out at a constant deposition potential of −1.5 V vs SCE for constant plating time. At the end of each deposition time, stripping analysis was performed immediately in the same plating bath (i.e., *in situ*) by sweeping the potential to more anodic potentials at a sweep rate of 10 mV s^{-1}. The structure of Co–W codeposited from the citrate bath on the steel cathode was examined by X-ray diffraction analysis using a Philips diffractometer (40 kV, 25 mA) with Ni filter and CuK_α radiation. The grain size (d) was estimated using the Sherrer equation:

$$d = \frac{0.9\lambda}{\beta \cos\theta} \tag{1}$$

where λ, β and θ are the wavelength of CuK_α (1.5406 Å), the integral width and the diffraction angle, respectively.

3. Results and discussion

3.1. *Potentiodynamic cathodic polarization curves*

In an effort to understand the mechanism of Co–W codeposition, the cathodic polarization curves involved in the deposition of Co–W alloys were traced and the results are given in Figures 1–4. Figure 1 illustrates the potentiodynamic cathodic polarization curves for the deposition of cobalt (curve a) and for the codeposition of Co–W alloy (curve b). However, curve c represents hydrogen discharge only, since W-alone cannot be deposited from pure aqueous solutions of sodium tungstate [2]. The curve of cobalt deposition and that of Co–W codeposition lie close to each other, especially at low current densities. This result is in agreement with the data reported by Holt et al. [19] in which the difference between the deposition of the alloy and the iron-group metals was very small (about 15 mV). The polarization curve of Co–W alloy exhibits a small limiting current plateau as a result of the deposition limitation by the diffusion process. The facilitation of the reduction of metals during alloy formation is connected with the change in the partial free energy of the alloy, which also increases the equilibrium potential [20].

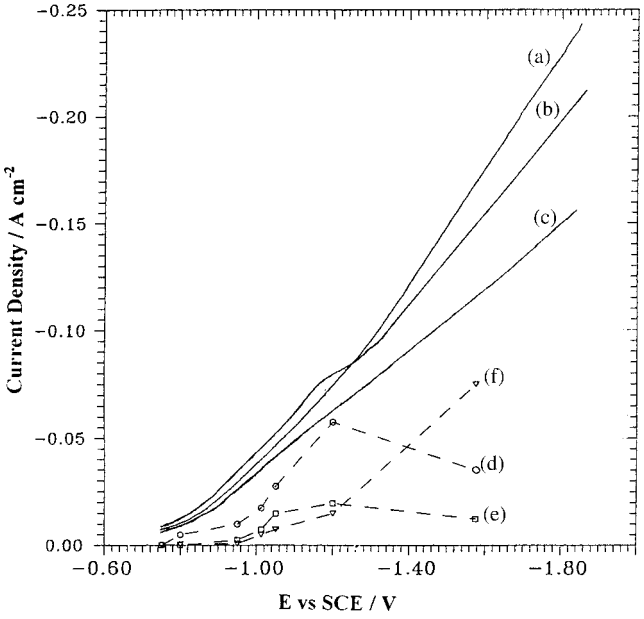

Fig. 1. Cathodic polarization curves: (a) Co from Co-1 bath, (b) Co–W alloy from (Co–W)* bath and (c) H_2 reduction from W-1 bath. Calculated curves: (d) for Co, (e) for W and (f) for Co–W alloy.

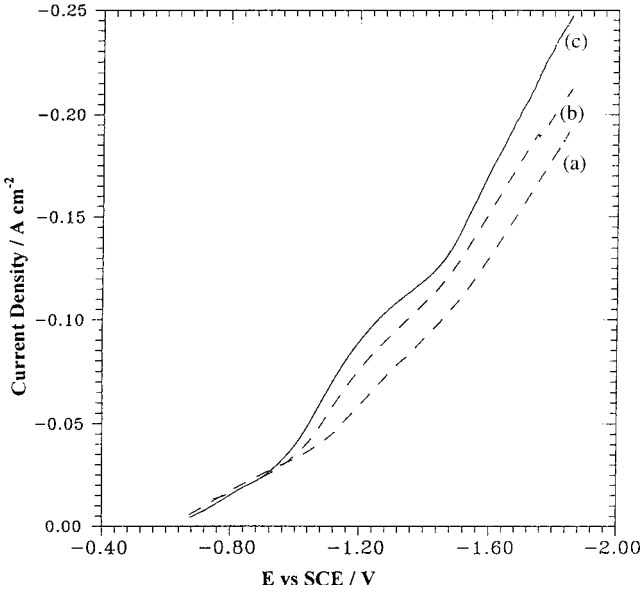

Fig. 2. Effect of $CoSO_4$ concentration of (Co–W)* bath on the potentiodynamic polarization curves of the alloy: (a) 0.14, (b) 0.20 and (c) 0.28 M.

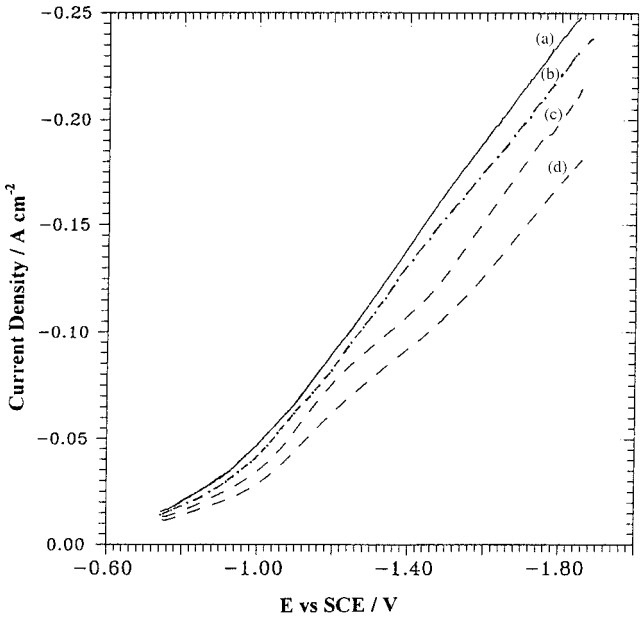

Fig. 3. Cathodic polarization curves of Co–W alloy codeposited from (Co–W)* bath at different pH: (a) 3.0, (b) 3.5, (c) 4.0 and (d) 5.5.

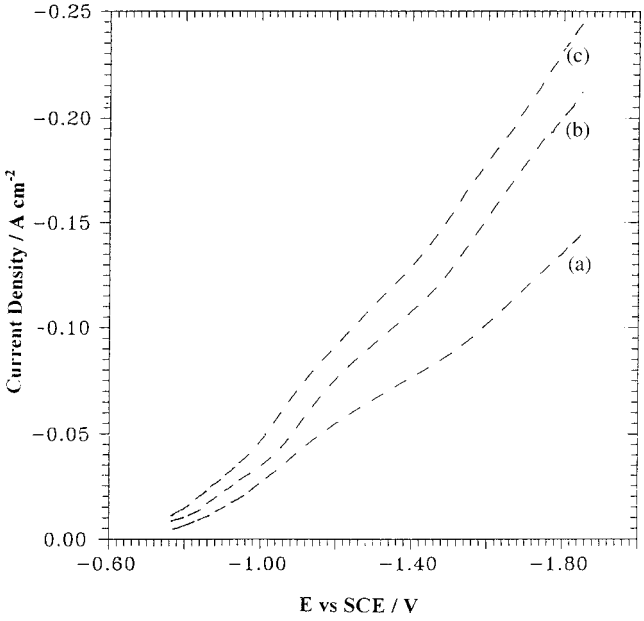

Fig. 4. Cathodic polarization curves of Co–W alloy codeposited from (Co–W)* bath at different temperatures; curves: (a) 25 °C, (b) 40 °C and (c) 50 °C.

It should be noted that Co–W codeposition is complicated by the simultaneous discharge of hydrogen ions, which occurs both during the separate electrodeposition of cobalt and during the codeposition of Co–W alloy. However, with the aid of the experimentally determined alloy compositions over the range of current density used, the actual (calculated) partial polarization curve for each component during codeposition could be computed [2]. Consequently, the polarization curve of the alloy deposition resolved into three component curves of partial current densities, two of them being Co and W could be calculated using Equation 2:

$$i_{\text{partial}} = i_{\text{alloy}} \times (\text{percentage metal in the alloy}) \qquad (2)$$

while the third component (H_2) could be evaluated using Equation 3:

$$i_{H_2} = i_{\text{total}} - (i_{\text{Co}} + i_{\text{W}}) \qquad (3)$$

The computed partial polarization curves of Co (curve d), W (curve e) and H_2 (curve f) are plotted in Figure 1 (the dotted curves). These calculated curves differ greatly from the corresponding experimental polarization curves for individual deposition. It is obvious from these data that the Co content in the deposit is expected to be higher than that of tungsten.

The effects of metal ion concentration, pH and temperature on the cathodic polarization of codeposition from baths containing sodium citrate and citric acid were determined. Figure 2 shows the effect of increasing Co^{2+} ion content on the potentiodynamic polarization curves of the alloy. The curves, as well as the codeposition potential, are shifted towards less negative potential values when the Co^{2+} ion content is increased. The small limiting current plateau of the polarization curve, increases with increasing Co^{2+} content as a result of the diffusion limitation of Co^{2+}. Similar experiments were carried out with varying tungstate concentration (at constant Co^{2+} content) and these results (not supplied here) show a slight effect of tungstate content on the cathodic polarization curves.

The effect of changing the pH (pH 3.0–5.5) on the potentiodynamic polarization curves is given in Figure 3. The bath pH has a large effect on the polarization curves and, consequently, on the deposition process. As the pH increases the polarization curves are shifted negatively and the limiting current becomes more pronounced.

The effect of temperature on the cathodic polarization curves for alloy codeposition is shown in Figure 4. The cathodic polarization decreases with increasing temperature. This behaviour may be attributed to a decrease in the activation polarization of the reducible species. Moreover, an increase in temperature enhances the concentration of the reducible species in the diffusion layer due to the increase in their diffusion coefficients.

From the above data it was found that the optimum bath composition for producing sound and satisfactory Co–W alloy contains: 0.2 M $CoSO_4$, 0.05 M Na_2WO_4, 0.04 M $C_6H_8O_7$ and 0.25 M $Na_3C_6H_5O_7$ and this bath is denoted as (Co–W)*.

The mechanism of induced codeposition proposed up to about 1960 was summarized by Brenner [2]. In the codeposition mechanism proposed so far, hypotheses have been advanced on the basis of the formation of an insoluble intermediate compound of partly reduced tungsten oxide.

The oxygen in Co–W alloy codeposited from the present citrate baths was determined by EDX. It seems that alloy formation takes place through (i) electrochemical reduction of tungstate ion to tungstate oxide or hydroxide, and (ii) chemical reduction of tungstate oxide to tungsten metal with hydrogen atoms bonded to the d-band vacancy of freshly deposited cobalt as shown in the following scheme:

$$WO_4^{2-} + 4H_2O + 2e^- \rightarrow WO_2 \cdot 2H_2O + 4OH^- \quad (4)$$

$$WO_2 \cdot 2H_2O + 4H\text{–}(Co) \rightarrow Co\text{–}W + 4H_2O \quad (5)$$

where H–(Co) indicates a hydrogen atom bonded to the d-band vacancy of cobalt. The importance of hydrogen in the formation of the induced codeposition was confirmed by Crousier et al. [21]. The tungsten content in the deposit is determined by both the catalytic ability of hydrogen attached on freshly deposited cobalt and the amount of intermediate tungsten oxide reduced from tungstate ions.

3.2. *Cathodic current efficiency and composition of Co–W alloys*

The cathodic current efficiency CCE of Co–W alloys codeposited from acid citrate baths is less than 100% as a result of simultaneous hydrogen evolution. The effect of bath composition and some plating parameters on the overall cathodic current efficiency CCE for the alloy deposition, as well as on the tungsten content in the deposits percentage W (w/w) were analysed and the results are given in Figures 5–9. In all cases it is noticeable that the W content in the deposit is always less than its content in the bath and it falls far below the composition-reference lines (CRL), which represent the per cent tungsten in the bath. These results imply that Co is the more readily depositable metal, as expected from the cathodic polarization data.

Figure 5 shows the effect of increasing Co^{2+} content on the cathodic current efficiency of the alloy codepo-

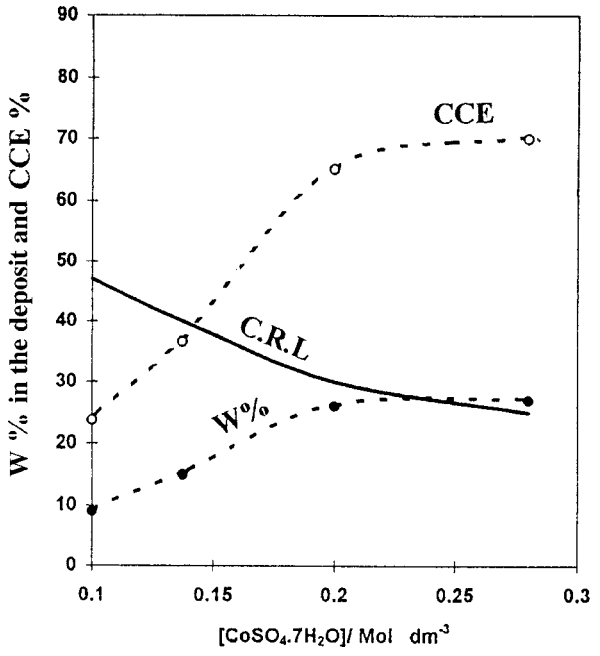

Fig. 5. Effect of $CoSO_4$ concentration on CCE and percentage of W in the deposits from (Co–W)* bath at $i = 3$ A dm^{-2}, pH 5.0, $t = 20$ min. and at 25 °C.

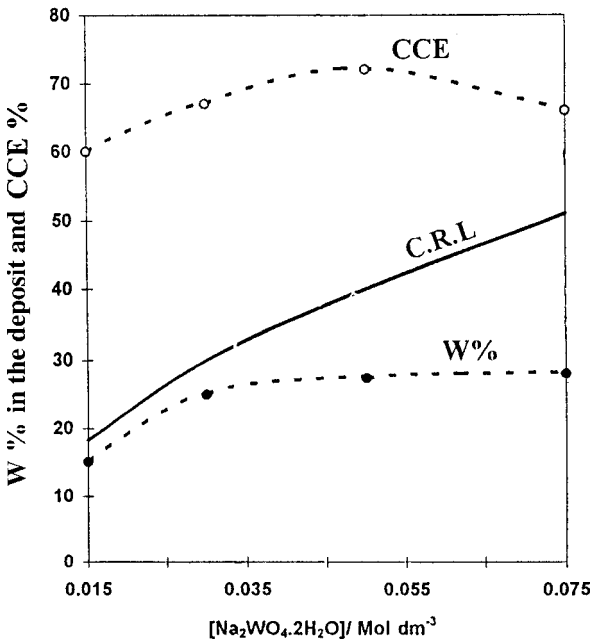

Fig. 6. Effect of Na_2WO_4 concentration on CCE and percentage of W in the deposits from (Co–W)* bath at $i = 3$ A dm^{-2}, pH 5.0, $t = 20$ min and at 25 °C.

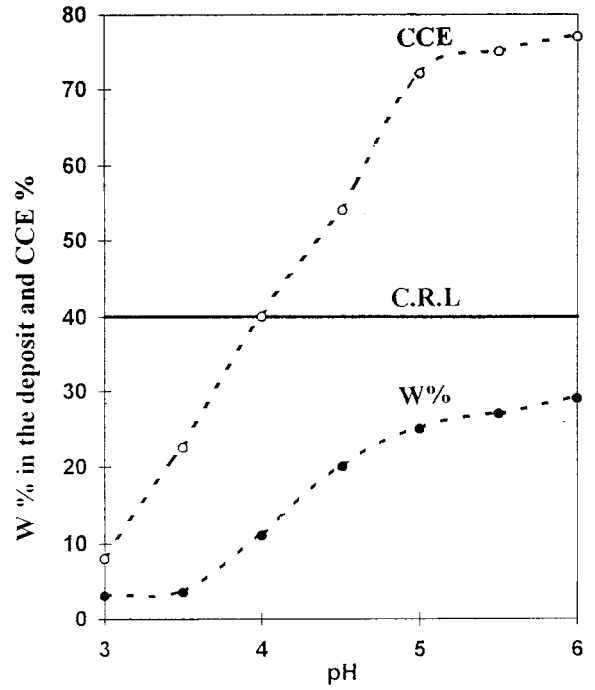

Fig. 7. Effect of bath pH on CCE and percentage of W in the deposits from (Co–W)* bath at $i = 3$ A dm^{-2}, $t = 20$ min and at 25 °C.

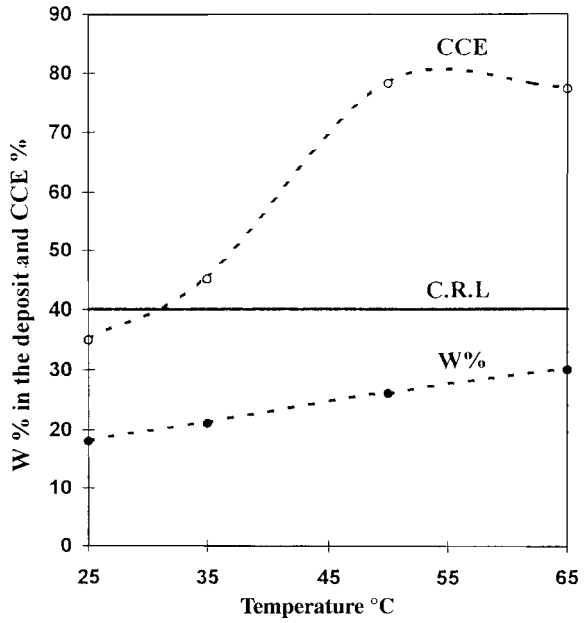

Fig. 8. Effect of temperature on CCE and on percentage of W in the deposits from (Co–W)* bath at $i = 3$ A dm^{-2}, $t = 20$ min. and pH 5.0.

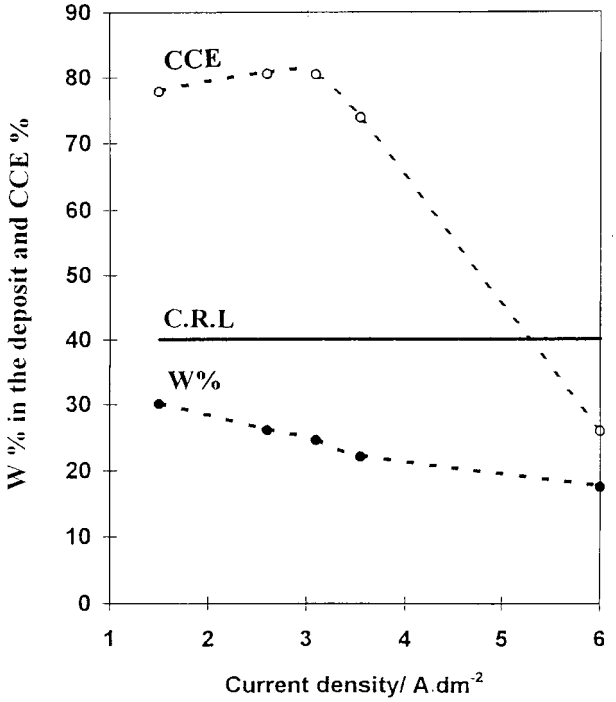

Fig. 9. Effect of current density on CCE and percentage of W in the deposits from (Co–W)* bath at pH 5.0, $t = 20$ min and at 25 °C.

sition as well as on the percentage W in the deposit. The cathode current efficiency CCE increases with increasing Co^{2+} content and then levels off at 70%. On the other hand, at low Co^{2+} content, the W content in the deposit was low (about 9%). However, with further increase in Co^{2+} content the W content in the deposit increases and reaches a maximum value of 28%. This confirms the induced codeposition of W in the presence of Co.

According to the equilibrium diagram data, the solubility of tungsten in cobalt, at room temperature, is about 13 at. % [22]. According to the present data Co–W alloys of 28% W could be obtained by electrodeposition.

The effect of tungstate ion content on the W content in the deposit and on the CCE is given in Figure 6. The CCE increases slightly, reaching a maximum value of 70%, and then decreases slightly, with increasing tungstate content in the bath. On the other hand, the tungsten content in the deposit increased with increasing tungstate ion content and then tends to level off at 28%, whatever the amount of tungstate added.

Figure 7 illustrates the influence of pH of the citrate bath on the current efficiency and on the W content in the deposit. It was found that the bath pH has a large effect on the CCE, as well as on the W content in the deposit. For example, increasing pH from 3.0 to 6.0 increases the W content in the deposit from 4 to 28%. At the same time the CCE increases from 8 to 78%. The decrease in CCE with decreasing pH may be attributed to the larger hydrogen ion concentration, resulting in evolution of larger amounts of hydrogen. It is noteworthy that as the pH increases the Co–W alloy becomes brighter, having a metallic luster as a result of increasing W content.

Bath temperature is an important variable in the operation of tungsten alloy codeposition, not only because of its effect on the W content of the deposit, which is rather small, but also because of its effect on the deposit soundness. An elevation of bath temperature improves the CCE of the alloy deposition up to 50 °C and then it tends to level off (Figure 8). The W content in the alloy slightly increases with increasing bath temperature in agreement with Brenner's observations [2]. The main benefit of an increase in bath temperature is the production of deposits having a more metallic appearance and an increase in the cathode current efficiency.

Figure 9 illustrates the influence of current density on the cathodic current efficiency CCE and on the W content in the deposit. The CCE is generally high at low current densities. On the other hand, the tungsten content decreases with increasing current density. However, further increase in current density (>3.3 A dm^{-2}) decreases the CCE significantly. This suggests that alloy formation through the reduction of intermediate tungsten oxide to the metallic state is depressed at high current density.

3.3. *Anodic stripping voltammetry*

The alloys were potentiostatically deposited on platinum sheet under different plating conditions at constant deposition potential for a constant time then anodic stripping analysis was performed immediately (*in situ*) in the same solution under the same conditions with a sweep rate of 10 mV s^{-1}. A typical anodic stripping responses of Co and Co–W alloy previously deposited at

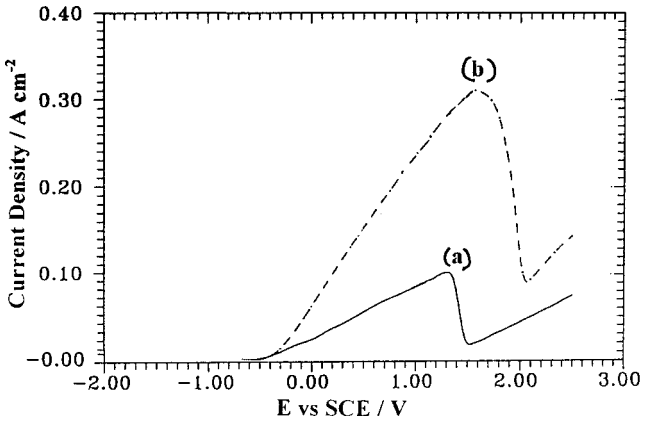

Fig. 10. Anodic linear stripping voltammetry curves: (a) Co deposited from Co-1 bath and (b) Co–W alloy codeposited from (Co–W)* bath.

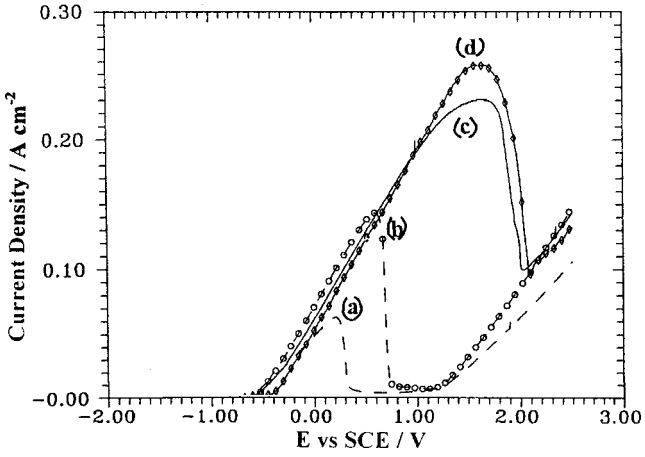

Fig. 11. Anodic linear stripping voltammetry curves of Co–W alloy codeposited from (Co–W)* bath with different concentrations of $CoSO_4$: (a) 0.1, (b) 0.14, (c) 0.20 and (d) 0.28 M.

pH 5.0 and at 25 °C are shown in Figure 10. The deposition was carried out at −1.5 mV for 360 s. Co–W alloy exhibits a very well defined anodic peak. In this case, the two components, Co and W, dissolve simultaneously so that the resulting voltammogram shows only one peak. The presence of a single anodic peak of alloy stripping denotes that the alloy consists of one phase (solid solution). Figure 11 shows that both the height and the area of the anodic peak corresponding to the dissolution of Co–W strongly depends on the concentration of Co^{2+} ions. Therefore, the anodic stripping results presented above indicate that this method could be employed successfully in *in situ* monitoring of the Co^{2+} concentration. On the other hand, the results show that the anodic stripping peak does not depend significantly on tungstate concentration.

Figure 12 shows the effect of pH on the peak height of the anodic stripping voltammetry. At low pH (pH 3.0) a very small anodic peak appears (curve a) indicating that the main reaction is the discharge of hydrogen ions. However, at higher pH values alloys are deposited in significant amounts.

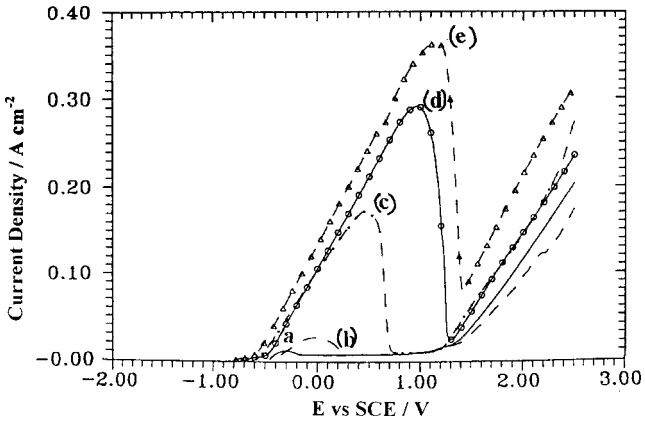

Fig. 12. Anodic linear stripping voltammetry curves of Co–W alloy codeposited from (Co–W)* bath with different pH: (a) 3.0, (b) 3.5, (c) 4.5, (d) 5.0 and (e) 5.5.

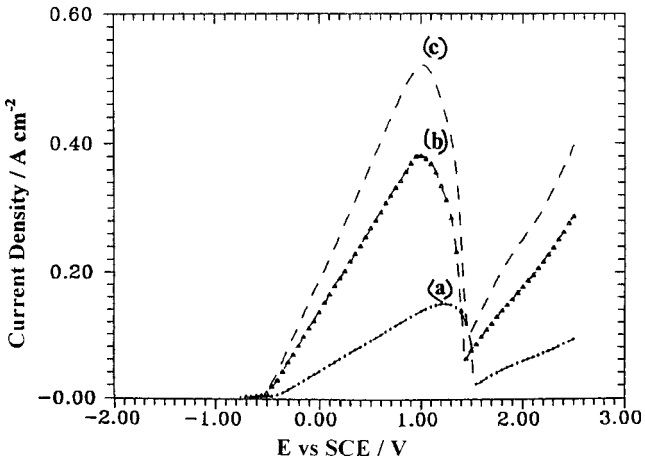

Fig. 13. Anodic linear stripping voltammetry curves of Co–W alloy codeposited from (Co–W)* bath at different temperatures: (a) 20, (b) 35 and (c) 50 °C.

The effect of temperature on the peak height of the anodic stripping voltammetry is shown in Figure 13. High temperature increases the peak height considerably. This means that the current efficiency increases with increasing temperature, in agreement with the previous polarization curves as well as with the alloy composition (Figure 4).

3.4. *X-ray measurements*

The deposited Co–W alloys obtained from citrate baths onto steel substrate are generally adherent, compact and smooth. The microstructure of the as-deposited Co–W alloy from the optimum (Co–W)* bath was tested by X-ray diffraction analysis. Figure 14 presents the X-ray pattern of Co–W alloy codeposited at pH 5.0 (percentage W ≡ 28%) which shows only a broad peak around 2θ of 75 deg and, suggests that the alloy deposit consists of a noncrystalline phase of estimated grain size 1 nm. Co–W alloys prepared by electrodepsoition are usually

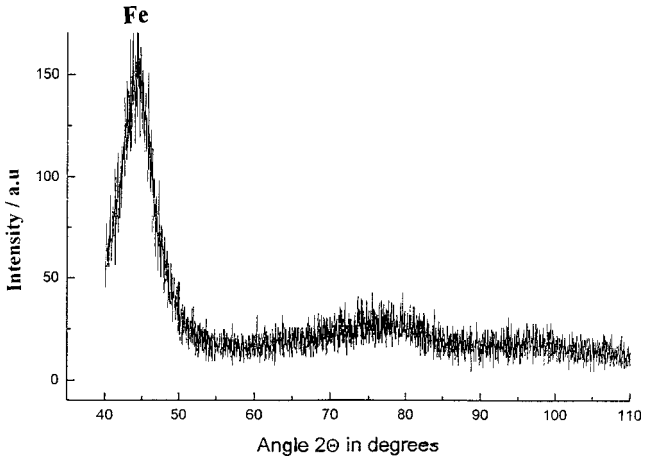

Fig. 14. X-ray diffraction pattern of as-deposited Co–W (W = 28%) alloy from (Co–W)* bath at $i = 3$ A dm^{-2}, pH 5.0, $t = 20$ min and at 25 °C.

amorphous and not crystalline [3, 10,11]. The Co–W structure was investigated in detail by Omi et al. [10] and it was suggested that the stoichometric composition of the alloy is Co_3W. The authors stated that the alloy consists of distinct basic tetrahedral units, each composed of three cobalt atoms and one tungsten atom. This tetrahedral arrangement comes from the fact that tungsten does not electrodeposit by itself from aqueous solutions [2] although cobalt and cobalt–tungsten do. The noncrystalline alloy structure must arise either because of deposition process produces mutually incoherent particles which are too small for the crystalline configuration to be formed energetically [23] or because the atoms do not bond together in the arrangement required for crystalline long-range order [10].

4. Conclusion

The induced electrodeposition of Co–W alloys onto steel substrates from acid citrate baths was carried out from an optimum bath containing: 0.2 M $CoSO_4$, 0.05 M Na_2WO_4, 0.04 M $C_6H_8O_7$ and 0.25 M $Na_3C_6H_5O_7$. Highly adherent, compact and very smooth deposits are obtained from this optimum bath. The computed partial polarization curves of Co, W and H_2 show that the Co content in the deposit is expected to be higher than that of tungsten in agreement with the results obtained by chemical analysis of the deposits. The percentage W (w/w) in the deposit increases with increasing either; pH, temperature or Co^{2+} ion concentration. With increasing current density the W% decreases. In each case the percentage W in the deposits never exceeds 28%. Anodic linear stripping voltammetry indicates that the alloy consists of one phase solid solution and these alloys are determined to be noncrystalline by X-ray diffraction analysis.

References

1. W.H. Safranek, 'The Properties of Electrodeposited Metals and Alloys' (American Elsevier, New York, 1974), p. 63.
2. A. Brenner, 'Electrodeposition of Alloys', Vol. 2 (Academic Press, New York, 1963).
3. M. Donten, T. Gromulski and Z. Stojek, *J. Alloys. Comp.* **279** (1998) 272.
4. R.M. Krishnan, C.J. Kennedy, S. Jayakrishnan, S. Sriveeraraghavan, S.R. Natarajan and P.G. Venkatakrishnan, *Met. Finish.* **93** (1995) 33.
5. E. Gileadi and O. Younes, *Electrochem. Solid-State Lett.* **3** (2000) 543.
6. M. Donten and Z. Stojek, *J. Appl. Electrochem.* **26**(6) (1996) 665.
7. C. Barnes, *Trans. IMF* **63**(2) (1985) 47.
8. J.K. Dennis, K.J. Lodge and F.A. Still, *Trans. IMF* **55** (1977) 17.
9. J.K. Dennis and F.A. Still, *Cobalt Abst. (Belgium)*, **1** (1975) 17.
10. T. Omi, H. Yamamoto and H.L. Glass, *J. Electrochem. Soc.* **119** (1972) 168.
11. K. Wikiel and J. Osteryoung, *J. Appl. Electrochem.* **22** (1992) 506.
12. M. Donten, H. Cesiulis and Z. Stojek, *Electrochim. Acta* **45** (2000) 3389.
13. N. Atanassov, K. Gencheva and M. Bratoeva, *Plat. Surf. Finish.* (1997) 67.
14. M.L. Holt and M.L. Nielsen, *Trans. Electrochem. Soc.* **82** (1942) 193.
15. D.W. Ernst and M.L. Holt, *J. Electrochem. Soc.* **105** (1958) 686.
16. M. Ishikawa, H. Enomoto, M. Matsuoka and C. Iwakwra, *Electrochim. Acta* **40** (1995) 1663.
17. A.R. Despic, V.D. Jovic and S. Spaic, *J. Electrochem. Soc.* **136** (1989) 1651.
18. M. Pushpavanam and K. Balakrishnan, *J. Appl. Electrochem.* **26** (1996) 1065.
19. M.L. Holt and R.E. Black, *US Patent* 2 432 894 (1947).
20. V.A. Averkin, 'Electrodeposition of Alloys' (Moskova, 1961), p. 8.
21. J. Crousier, M. Eyraud, J.-P. Crousier and J.-M. Roman, *J. Appl. Electrochem.* **22** (1992) 749.
22. W. Koester and W. Tonn, *Z. Metallkunde* **24** (1932) 296.
23. T. Omi, H.L. Glass and H. Yamamoto, *J. Electrochem. Soc.* **123** (1976) 341.